Mitochondrion 49 (2019) 97–110

Contents lists available at ScienceDirect

Mitochondrion

journal homepage: www.elsevier.com/locate/mito

Original Research Article

Upregulated PDK4 expression is a sensitive marker of increased fatty acid oxidation

Ina Katrine Nitschke Pettersen[a,1], Deusdedit Tusubira[a,1], Hanan Ashrafi[a], Sissel Elisabeth Dyrstad[a], Lena Hansen[a,b], Xiao-Zheng Liu[a], Linn Iren Hodneland Nilsson[a], Nils Gunnar Løvsletten[c], Kjetil Berge[d], Hege Wergedahl[e], Bodil Bjørndal[f], Øystein Fluge[b], Ove Bruland[g], Arild Christian Rustan[c], Nils Halberg[a], Gro Vatne Røsland[a,b], Rolf Kristian Berge[f,h], Karl Johan Tronstad[a,*]

[a] Department of Biomedicine, University of Bergen, Norway
[b] Department of Oncology and Medical Physics, Haukeland University Hospital, Bergen, Norway
[c] Department of Pharmacy, University of Oslo, Norway
[d] Skretting AS, Stavanger, Norway
[e] Department of Sport, Food and Natural Sciences, Western Norway University of Applied Sciences, Bergen, Norway
[f] Department of Clinical Science, University of Bergen, Norway
[g] Department of Medical Genetics and Molecular Medicine, Haukeland University Hospital, Bergen, Norway
[h] Department of Heart Disease, Haukeland University Hospital, Bergen, Norway

ARTICLE INFO

Keywords:
Metabolic regulation
Metabolic flexibility
Fatty acid oxidation
Mitochondria
Cell metabolism
Biomarker
Pyruvate dehydrogenase kinase
Peroxisome proliferator-activated receptor (PPAR)

ABSTRACT

Fatty acid oxidation is a central fueling pathway for mitochondrial ATP production. Regulation occurs through multiple nutrient- and energy-sensitive molecular mechanisms. We explored if upregulated mRNA expression of the mitochondrial enzyme pyruvate dehydrogenase kinase 4 (PDK4) may be used as a surrogate marker of increased mitochondrial fatty acid oxidation, by indicating an overall shift from glucose to fatty acids as the preferred oxidation fuel. The association between fatty acid oxidation and PDK4 expression was studied in different contexts of metabolic adaption. In rats treated with the modified fatty acid tetradecylthioacetic acid (TTA), *Pdk4* was upregulated simultaneously with fatty acid oxidation genes in liver and heart, whereas muscle and white adipose tissue remained unaffected. In MDA-MB-231 cells, fatty acid oxidation increased nearly three-fold upon peroxisome proliferator-activated receptor α (PPARα, *PPARA*) overexpression, and four-fold upon TTA-treatment. *PDK4* expression was highly increased under these conditions. Further, overexpression of *PDK4* caused increased fatty acid oxidation in these cells. Pharmacological activators of PPARα and AMPK had minor effects, while the mTOR inhibitor rapamycin potentiated the effect of TTA. There were minor changes in mitochondrial respiration, glycolytic function, and mitochondrial biogenesis under conditions of increased fatty acid oxidation. TTA was found to act as a mild uncoupler, which is likely to contribute to the metabolic effects. Repeated experiments with HeLa cells supported these findings. In summary, PDK4 upregulation implies an overarching metabolic shift towards increased utilization of fatty acids as energy fuel, and thus constitutes a sensitive marker of enhanced fatty acid oxidation.

Abbreviations: ACC, acetyl-CoA carboxylase; ACOX, acyl-CoA oxidase 1; AICAR, 5-aminoimidazole-4-carboxamide ribonucleotide; AMPK, AMP-dependent protein kinase; CCCP, carbonyl cyanide 3-chlorophenylhydrazone; COX4I1, cytochrome *c* oxidase subunit IV; CPT, carnitine palmitoyltransferase; ECAR, extracellular acidification rate; GFP, green fluorescence protein; ME-1, malic enzyme 1; mTOR, mammalian target of rapamycin; NRF1, nuclear respiratory factor 1; OCR, oxygen consumption rate; PA, palmitic acid; PDH, pyruvate dehydrogenase; PDK, pyruvate dehydrogenase kinase; PPAR, peroxisome proliferator-activated receptor; TFAM, mitochondrial transcription factor A; TTA, tetradecylthioacetic acid; WAT, white adipose tissue; WY 14,643, 4-Chloro-6-(2,3-xylidino)-2-pyrimidinylthioacetic acid

* Corresponding author at: Department of Biomedicine, University of Bergen, Jonas Lies vei 91, N-5009 Bergen, Norway.
E-mail address: karl.tronstad@uib.no (K.J. Tronstad).

[1] Equal contribution.

https://doi.org/10.1016/j.mito.2019.07.009
Received 12 April 2019; Received in revised form 1 July 2019; Accepted 24 July 2019
Available online 25 July 2019

1. Introduction

Mitochondrial fatty acid oxidation is a crucial and highly regulated fueling pathway for aerobic ATP production in mammalian organisms. Abnormalities of mitochondrial fatty acid oxidation affects diverse cellular and systemic functions, and have been linked to conditions such as diabetes, metabolic syndrome, cancer, cancer cachexia, neurodegeneration and ME/CFS (Naviaux et al., 2016; Germain et al., 2017; Rohlenova et al., 2018; Adeva-Andany et al., 2018; Fukawa et al., 2016). Functional analysis of mitochondrial fatty acid oxidation in conventional biopsies are difficult, partly since it requires viable cells or non-frozen tissue samples. Identification of sensitive and effective surrogate markers of mitochondrial fatty acid oxidation may thus provide new opportunities to assess (patho)physiological effects on metabolism. Fatty acid catabolism is co-regulated with other pathways of cell metabolism to support homeostasis when the energy supply or demand change. There is a well-established concept of reciprocal regulation between fatty acid and glucose oxidation for energy purposes. Different types of metabolic adaptations may occur to accommodate (patho) physiological changes (Sugden and Holness, 1994; Trexler et al., 2014; Jose et al., 2013). The pyruvate dehydrogenase (PDH) complex and the carnitine palmitoyltransferase (CPT) system are important in this context. PDH converts pyruvate from glycolysis to acetyl-CoA and CO_2 through oxidative decarboxylation, whereas the CPT system transports fatty acids into mitochondria, a rate-limiting process for acetyl-CoA production by mitochondrial fatty acid oxidation. PDH and the CPT system are both regulated in response to changing energy conditions, partly through contextual nutrient-gene and nutrient-protein interactions that leads to metabolic adaptations. Increased rates of fatty acid oxidation, e.g. due to starvation or insulin-deficient diabetes, is associated with suppression of PDH activity (reviewed in (Holness and Sugden, 2003)). This is important for conserving 3-carbon precursors for glucose synthesis when glucose is scarce. Such long-term adaptive effect on PDH activity status can partly be explained by altered expression of PDH kinases (PDKs), which phosphorylate and inhibit the PDH complex (Holness and Sugden, 2003). There are four PDK isoenzymes, PDK1–4, all expressed in a tissue-specific manner (reviewed in (Jeong et al., 2012)). As suggested by Holness and Sugden, the PDKs may be considered to act as tissue homeostats supporting adequate context-dependent regulation of energy fueling pathways (Holness and Sugden, 2003). In particular, changed PDK4 expression appears to play an important role in lipid-related metabolic adaptations in various tissues (reviewed in (Holness and Sugden, 2003; Sugden, 2003; Roche and Hiromasa, 2007)). Increased level of PDK4, e.g. due to starvation (Wu et al., 2000), favors inactivation of PDH in oxidative tissues, and thereby implements an influential metabolic shift from glucose to fatty acid oxidation. Furthermore, under such conditions, reduced production of malonyl-CoA, an important inhibitor of mitochondrial fatty acid uptake and oxidation (the CPT system), will support increased rates of fatty acid oxidation.

Fatty acid oxidation is also controlled by nutrient- and energy-sensitive factors, such as AMP-dependent protein kinase (AMPK), the family of peroxisome proliferator-activated receptor transcription factors (PPARs) and the mammalian target of rapamycin (mTOR) (recently reviewed in (Desvergne et al., 2006; Lin and Hardie, 2018; Saxton and Sabatini, 2017)). The PPAR family consists of three main isoforms (PPARα, PPARδ, PPARγ), among which PPARα is a central regulator of context-dependent changes in fatty acid oxidation (Desvergne et al., 2006). AMPK is activated by a low cellular energy state, which commonly leads to increased mitochondrial biogenesis and stimulated oxidation rates (Hodneland Nilsson et al., 2015; Tronstad et al., 2014). AMPK also inactivates acetyl-CoA carboxylase (ACC), which is an enzyme producing malonyl-CoA (Winder et al., 1997; O'Neill et al., 2014). Pharmacological activation of AMPK with 5-aminoimidazole-4-carboxamide ribonucleotide (AICAR) causes increased fatty acid oxidation in rat muscle (Merrill et al., 1997). In contrast to PPARα and AMPK, the activity of mTOR primarily supports biosynthesis rather than catabolism. Hence, in an energy-limited context, e.g. glucose deprivation, increased rates of mitochondrial fatty acid oxidation may be supported by multiple regulatory events, including PPARα and/or AMPK activation, and mTOR inhibition. The contextual effects depend on both the type of trigger as well as cell-specific properties regarding the contributing signaling factors and their downstream mediators, such as PDKs. These mechanisms regulate both the activity balance between glucose and fatty acid oxidation, and the ability to switch between these fueling pathways, a trait often referred to as metabolic flexibility (Galgani et al., 2008).

PDK4 is normally highly expressed in tissues with high energy demand, including heart, skeletal muscle, liver, kidney, pancreatic islet and lactating mammary gland (Holness and Sugden, 2003; Wu et al., 2000). In these tissues, PDK4 expression is typically induced when the blood free fatty acid level increases, such as during starvation; and this is mediated partly through PPARα, but also by other mechanisms (Jeong et al., 2012; Sugden et al., 2001). PPARα-agonists, such as WY-14,643, have been found to significantly induce PDK4 expression in rat muscle (Wu et al., 1999), and PDK4 upregulation through PPARα may be involved in cancer cachexia (Pin et al., 2019). Further, PDK4 was reported to be highly upregulated upon cardiac-restricted overexpression of PPARα in mice, and this was associated with increased myocardial fatty acid oxidation rates (Finck et al., 2002). Upregulation of PDK4 was also found in adipocytes after treatment with the PPARγ-selective activator rosiglitazone, but not liver and muscle (Cadoudal et al., 2008). In muscle cells, PPARδ was found to mediate contextual upregulation of PDK4 (Badin et al., 2012; Feng et al., 2014). Although AMPK and mTOR are known to respond to low energy conditions, there are few reports on how these factors may affect the relationship between PDK4 and fatty acid oxidation e.g. upon starvation. Combined activation of AMPK and PPARδ caused increased *Pdk4* expression in mouse muscle, and this was associated with increased fat oxidation during prolonged exercise (Manio et al., 2016). The hypolipidemic modified fatty acid tetradecylthioacetic acid (TTA) is known to act through multiple mechanisms to induce mitochondrial fatty acid oxidation in cells and animals, both dependent and independent of PPARs (Berge et al., 2005; Rost et al., 2009; Grav et al., 2003; Wensaas et al., 2009). Potential effects of TTA on PDK4 expression have not yet been reported.

Based on current knowledge, increased PDK4 expression appears to imply a coordinated metabolic shift from glucose to fatty acids as major energy fuel. The present study was undertaken to solidify the relationship between PDK4 expression and fatty acid oxidation, by pursuing in vivo findings through extensive investigations of context-dependent metabolic functions in living cells.

2. Materials and methods

2.1. Rat model

The rat study was part of a larger study previously reported (Vigerust et al., 2012). The protocol was approved by the Norwegian State Board of Biological Experiments with Living Animals. Ten weeks old male Wistar rats (200–250 g) were obtained from Taconic Europe. After one week of acclimatization, the control group was fed on high fat diet (23% lard + 2% soybean oil), and treatment group was given the same diet supplemented with TTA (0.375%) for 50 weeks. The diets were isocaloric (energetic value 4900 Kcal). Animals were anaesthetized and sacrificed under non-fasting condition. Blood was drawn by cardiac puncture. All tissues were stored in liquid nitrogen before analysis. Further information is provided in (Vigerust et al., 2012).

2.2. Cell culture

All cell cultures were incubated at 37 °C (5% CO_2 in air).

Compounds and materials were from Sigma-Aldrich (St. Louis, MO, US), and catalogue numbers refers to products from this company, unless otherwise stated. MDA-MB-231 and HeLa cells were cultured in DMEM (4.5 g/l glucose, #D5671) supplemented with 10% heat-inactivated fetal bovine serum (FBS, #SH30079.03, GE Healthcare Hyclone), 50 μg/ml penicillin/streptomycin (#P-0781) and 2 mM L-glutamine.

2.3. Overexpression of PPARA and PDK4

For the overexpression of *PPARA*, a double-stranded DNA fragment (g-Block) encoding human *PPARA* and containing BamHI and *Sal*I restriction enzymes cutting sites was synthesized by Integrated DNA Technologies (IDT, Coralville, IA, US). The g-block fragment was then subcloned into the pBABE-puro (Addgene, plasmid 1764) retroviral vector with a puromycin resistance gene. An empty pBABE-puro vector was used as a control. HEK293T packaging cells were transfected with the retroviral vector and packaging vectors by Lipofectamine-2000 transfection (#11668–019, Thermo Fisher Scientific, Waltham, MA, US), following the manufacturer's instructions. At 5 h post-transfection, the medium was replaced with 10 ml fresh DMEM supplemented with 10% FBS. Virus were harvested after 24 h post-transfection. For retroviral infection, MDA-MB-231 cells were seeded in a 10-cm dish and infected with virus in the presence of polybrene (8 μg/ml). Cells were selected by puromycin (2 μg/ml) 48 h post infection.

For the overexpression of *PDK4*, A MMLV retrovirus gene expression vector containing *PDK4* cDNA (NM_002612) and *Bsd*, the blasticidine resistance gene (Kimura et al., 1994) was acquired from VectorBuilder (VectorBuilder Inc. 150 Pine Forest Drive, Suite 803, Shenandoah, TX 77384). HEK293 derived Phoenix-AMPHO (ATCC® CRL-3213™) packaging cells were transfected with the retroviral vector by Lipofectamine-2000 transfection, following the manufacturer's instructions. Stably transfected virus producing packaging cells were selected in DMEM medium containing 10 μg/ml blasticidin (#ant-bl-05, InvivoGen, 5, rue Jean Rodier F-31400 Toulouse, France), as described by others (Pear et al., 1993). For retroviral infection, MDA-MB-231 cells were seeded in 6-well plates and infected with virus in the presence of protamine sulfate (5 μg/ml). Cells were selected by blasticidin (10 μg/ml) 72 h post infection.

2.4. Cell culture treatment conditions

To investigate long-term effects (6 days) of metabolic modulators, 250,000 cells were plated in T75 flasks and incubated overnight to allow proper attachment. Final concentrations of 5-aminoimidazole-4-carboxamide 1-β-D-ribofuranoside (AICAR, 0.5 mM, Toronto Research Chemicals Inc., North York, ON, Canada), rapamycin (50 nM), tetradecylthioacetic acid (TTA, 30 μM and 60 μM, Synthetica AS, Oslo, Norway), 4-Chloro-6-(2,3-xylidino)-2-pyrimidinylthioacetic acid (WY 14,643, 10 μM) and vehicle (DMSO, 60 μM) were added to respective flasks. On day 3, the medium was replaced, and treatment continued. On day 5, the cells were re-plated at optimized cell densities for subsequent analyses the next day (day 6).

2.5. Extracellular flux analysis to study cell metabolism

Extracellular flux analysis was performed with the Seahorse XF^{e}96 Analyzer (Agilent, Santa Clara, CA, US). This simultaneously measures the oxygen consumption rate (OCR) and extracellular acidification rate (ECAR) in the medium directly above adherent cells. The experiments were performed according to standard protocols, and cell number and compound concentrations were optimized for each cell type. Cells were seeded in 96-well assay plates (Hela; 20,000, MDA-MB-231; 30,000 cells/80 μl/well) and let adhere overnight (5% CO_2 in air, 37 °C). The next day, growth medium was replaced with assay medium (un-buffered, phenol red-free DMEM, #D5030) supplemented for mitochondrial respiration assay with 10 mM glucose, 2 mM sodium pyruvate, 4 mM L-glutamine, pH 7.4, and for glycolysis assay with 4 mM glutamine, pH 7.4. After 1 h incubation in the Prep Station (37 °C, CO_2-free, Agilent) the plate was placed in the Seahorse XF^{e}96 Analyzer. Chemical modulators were injected sequentially to obtain metabolic flux profiles. For the mitochondrial respiration assay the final concentration of the modulators were 3 μM oligomycin, 1 μM CCCP, 1 μM rotenone and 1 μM antimycin A. For the glycolysis assay, final concentrations of 10 mM glucose, 3 μM oligomycin and 100 mM 2-deoxyglucose were added.

To study acute effects of palmitic acid (PA) and its modified analogue TTA, the cells (untreated) were seeded according to standard protocol (described above). The fatty acids (dissolved in DMSO) were added at specified concentrations (final concentrations: 30, 60, 100 and 200 μM) to the mitochondrial respiration assay medium immediately before inserting the plate into the Seahorse XF^{e}96 Analyzer.

When relevant, data were normalized to protein content, measured using the Pierce® BCA Protein Assay Kit (Thermo Fisher Scientific, Waltham, MA, US).

2.6. Substrate oxidation assay by $^{14}CO_2$-trapping

Substrate oxidation was assessed by providing the radiolabeled (^{14}C) substrate of interest to the cells, accompanied by trapping of the released $^{14}CO_2$; a technique previously described in (Wensaas et al., 2007). Cells were seeded in 96-well CellBind® microplates (MDA-MB-231; 45,000, HeLa; 40,000 cells/well) in DMEM and incubated overnight to allow proper attachment. The radiolabeled substrate of interest, either [1-^{14}C]pyruvic acid (0.25 μCi/ml), D-[^{14}C(U)]glucose (2 μCi/ml for MDA-MB-231, 4 μCi/ml for HeLa) or [1-^{14}C]palmitic acid (1 μCi/ml), all from PerkinElmer (Waltham, MA, US), was given in DPBS (with $MgCl_2$ and $CaCl_2$, #D8662) supplemented with 10 mM HEPES and 10 μM BSA. L-carnitine (1 mM) and glucose (0.5 mM) were included in the assay medium for palmitic acid oxidation. Respective amounts of non-radiolabeled substrate were added to obtain final concentrations of sodium pyruvate (0.2 mM or 2 mM), glucose (5 mM) and BSA-conjugated palmitic acid (100 μM), as indicated in the figures. For uncoupled substrate oxidation, the optimized concentration of CCCP (1 μM for pyruvate and glucose oxidation, 3 μM for palmitic acid oxidation) was added to the medium. The optimal CCCP concentration was higher for palmitic acid oxidation compared to the others due to the increased amount of BSA, which binds hydrophobic molecules. Etomoxir (40 μM) was added to selected wells during palmitic acid oxidation, to monitor the contribution of non-mitochondrial CO_2 production, which usually was 10–20% of basal activity (data not shown). The $^{14}CO_2$ trapping was performed as described (Wensaas et al., 2007). In brief, an inverted UniFilter®-96w GF/B microplate (PerkinElmer), activated for CO_2 capture with 1 M NaOH, was sealed to the top of the 96-well CellBind® cell culture microplate, and incubated for the indicated period of time at 37 °C. Subsequently, scintillation liquid (30 μl, Ultima Gold XR or MicroScint PS PerkinElmer) was added to the filters and the filterplate sealed with a TopSealA (PerkinElmer). Radioactivity was measured using a microplate scintillation counter (TopCount NXT, Packard, Meriden, CT, US or the MicroBeta^2 Microplate Counter, PerkinElmer). Protein measurement was performed for data normalization. The cells were washed twice with PBS, lysed (0.1 M NaOH), and measured using Pierce® BCA Protein Assay Kit (Thermo Fisher Scientific).

2.7. Gene expression by qPCR assays

Gene expression analysis in animal tissues was done as previously reported (Vigerust et al., 2012; Lindquist et al., 2017; Dyrstad et al., 2018). RNA was isolated from frozen tissues stored at −80 °C. In cell culture experiments, the cells were washed with PBS, pelleted and stored at −80 °C. Cellular RNA was extracted using the RNeasy mini kit including DNase digestion (RNase-Free DNase) (QIAGEN, Venlo,

Netherlands). Total RNA (50 ng/μl) was estimated by the use of a Nanodrop ND-1000 Spectrophotometer (NanoDrop Technologies, Boston, MA, US) and reversely transcribed using the Applied Biosystem's High Capacity cDNA Reverse Transcription Kit (Thermo Fisher Scientific) according to manufacturer instructions. All probes were obtained from Applied Biosystems unless otherwise stated. Probes used were: Acyl-CoA oxidase 1, (*ACOX* Human: Hs01074241, *Acox* Rat: Rn01460628), Cytochrome c oxidase subunit IV *(COX4I1* Human: Hs00971639), Carnitine palmitoyltransferase 1A *(Cpt1a* Rat: Rn00580702, *CPT1A* Human: Hs00912671), Carnitine palmitoyltransferase 1B (*Cpt1b* Rat: Rn00682395), Carnitine palmitoyltransferase 2 (*Cpt2* Rat: Rn00563995), Pyruvate dehydrogenase kinase 4 (*Pdk4* Rat: Rn00585577_m1, PDK4 Human: Hs01037712), Peroxisome proliferator activated receptor α (*PPARA* Human: Hs00947536), Malic enzyme-1 (*Me-1* Rat: Rn00561502_m1, *ME-1* Human: Hs00159110), Mitochondrial transcription factor A (*Tfam* Rat: Rn00580051_m1, *TFAM* Human: Hs01082775) and Nuclear respiratory factor (*Nrf* Rat: Rn01455960_m1). The reaction mixtures were loaded into a LightCycler® 480 Multiwell Plate 384 (Roche, Basel, Germany) by the Mosquito HV® low volume pipetting instrument (TTP Labtech Ltd., UK) (Dyrstad et al., 2018). The qPCR was run in a LightCycler 480 system (Roche, Basel, Germany) with the "Dual Color Hydrolysis probe – UPL Probe 384-11" instrument template-program. The expression level of each gene was calculated as fold change based on the delta delta Ct method (Livak and Schmittgen, 2001) and was normalized against 18S rRNA (Rat: RT-CKFT-18S from Eurogentec, Seraing, Belgium, Human: Eukaryotic 18S rRNA Endogenous Control, 4310893E).

2.8. Protein expression by western blotting

The cell pellets were lysed in RIPA lysis buffer (#sc24948, Santa Cruz Biotechnology, Dallas, TX) following the manufactures instructions. Pierce® BCA Protein Assay Kit (Thermo Fisher Scientific) was used to measure protein concentration in the lysates. The protein lysate mixed together with XT Sample Buffer (#1610791, Bio-Rad) were heated at 95 °C for 5 min, before 10–12 mg protein was loaded per well. The electrophoresis was done using Mini-PROTEAN® TGX™ Protein Gels, 4–20% gradient, running buffer (#1610772, Bio-Rad) and Bio-Rad Mini Protean 3 cell system (90 V for 15 min, 110 V for 1 h). The BioradTurbo Transfer System (2.5A, 25 V, 7 min) was used to transfer (transfer buffer, #1610734, Bio-Rad) the proteins onto the activated (30 s in metanol) polyvinylidene fluoride (PVDF) membrane (Trans-Blot® Turbo™ Mini-size LF PVDF). The membranes were blocked, for 1 h in room temperature, in Odyssey Blocking Buffer (TBS) (LI-COR Biosciences) before labeled with anti-PDK4 antibody (#ab11033, mouse monoclonal [1C2BG5], Abcam) diluted 1:500 in blocking buffer overnight at 4 °C. Anti-GAPDH antibody (#60004–1, mouse monoclonal, Proteintech) at a dilution of 1:1000 was used as loading control. After washing in TBS-T buffer the membranes were incubated for 2 h in IRDye® 800CW Goat anti-Mouse IgG secondary antibody (1:20000) (#P/N 926–32,210, LI-COR Bioscience). The protein bands were visualized using the 800 nm IRlong channel in the Amersham Typhoon Gel and Blot Imaging Systems (GE healthcare). Amersham™ Imager 600 software was used to view and analyze the blot images together with ImageJ software.

2.9. Live-cell reporter strategy to monitor mitochondrial biogenesis

Mitochondrial biogenesis was measured using a GFP-based live-cell reporter strategy previously described in (Hodneland Nilsson et al., 2015). Briefly, a reporter construct (NRF1mitoGFP) with mitoGFP under the control of a promoter with NRF-1 responsive element was inserted into HeLa (HeLaNRF1/c4) and MDA-MB-231 (MDA-MB-231/NRF1) cells. Following the treatment, the cellular expression of mitoGFP (fluorescence intensity) was measured as a readout of mitochondrial biogenesis. The cells were treated as indicated for 6 days, before they were trypsinized, washed with PBS and kept on ice until analyzed by flow cytometry (AccuriTM C6, BD Accuri Cytometers Inc., Ann Arbor, MI, US). The data were analyzed by FlowJo software.

2.10. Plasma lactate and glucose measurements

Biosen C-Line GP + (EKF Diagnostics, Cardiff, UK) was used to measure glucose and lactate concentrations in rat plasma, according to manufacturer's instructions.

2.11. Statistical analysis

All data were analyzed using Graphpad Prism 8 software (GraphPad Software; San Diego, CA, US). Results are shown as mean ± SD. ANOVA and student's *t*-test were used to evaluate statistical differences between the interventions and control. Pearson's correlation coefficients were used when comparing two independent variables. $P < .05$ was considered statistically significant.

3. Results

3.1. Pdk4 expression is a sensitive indicator of mitochondrial fatty acid oxidation in rat tissues

Increased hepatic fatty acid oxidation is established as an important mechanism behind the hypolipidemic effects of the modified fatty acid TTA in rats (Berge et al., 2005). In multiple studies, upregulated fatty acid oxidation has been demonstrated, both based on gene expression and enzymatic activity, most extensively in liver, but also in heart (Berge et al., 2005; Vigerust et al., 2012; Oie et al., 2013; Turell, 1989). In the present study, we used TTA-treatment as a model to evaluate the relationship between *Pdk4* mRNA expression and fatty acid oxidation *in vivo*. Gene expression was measured in tissue samples from a previous experiment in rats, where rats were treated with TTA for 50 weeks (Vigerust et al., 2012). *Pdk4* expression was compared with the expression of genes related to fatty acid oxidation in liver, heart, skeletal muscle and white adipose tissue (Fig. 1A, and Supplementary Fig. S1). In the liver of TTA-treated rats, the level of *Pdk4* mRNA increased 18-fold (18.0 ± 2.6), compared to control rats. This was associated with increased hepatic expression of *Cpt1a* (liver isoform, 2.4 ± 0.8), *Cpt2* (5.1 ± 1.2), and the classical PPARα target gene *Acox* (10.1 ± 2.8), supporting previous findings (Vigerust et al., 2012). Interestingly, TTA-treatment caused a potent increase in the expression of the muscle isoform *Cpt1b* in liver (487.1 ± 195.4), which has not previously been reported. The hepatic expression of *Tfam* was increased (2.4 ± 1.1) suggesting that elements of mitochondrial biogenesis may be involved, although *Nrf1* was not affected. We also analyzed the expression of cytosolic malic enzyme *Me-1* due to its interactions in pyruvate metabolism, as well as fatty acid oxidation by mediating TCA anaplerotism (Gibala et al., 2000; Carley et al., 2015). TTA-treated rats presented significantly increased expression of *Me-1* in liver (58.0 ± 21.9). In heart, a moderate induction of *Pdk4* (2.5 ± 0.7) was accompanied by relatively small, but statistically significant, increases in *Cpt1b* (1.2 ± 0.1), *Acox* (1.7 ± 0.3) and *Me-1* (1.5 ± 0.3) mRNA levels, and a small reduction in *Tfam* (0.8 ± 0.04), whereas the other transcripts remained unchanged. None of these genes were significantly affected in skeletal muscle or white adipose tissue in TTA-treated rats compared to controls. Plasma glucose and lactate levels were measured to evaluate how this long-term adaptation of oxidative metabolism affected systemic glucose homeostasis (Fig. 1B-C). While no effect was found for plasma lactate, the plasma glucose levels tended to be slightly lower in TTA-treated rats compared to controls, although this effect did not reach statistical significance. In summary, TTA-treated rats presented regulatory effects on fatty acid oxidation genes in agreement with a significant induction in liver and a moderate induction in heart, supporting previous measurements (Berge et al., 2005; Oie et al., 2013).

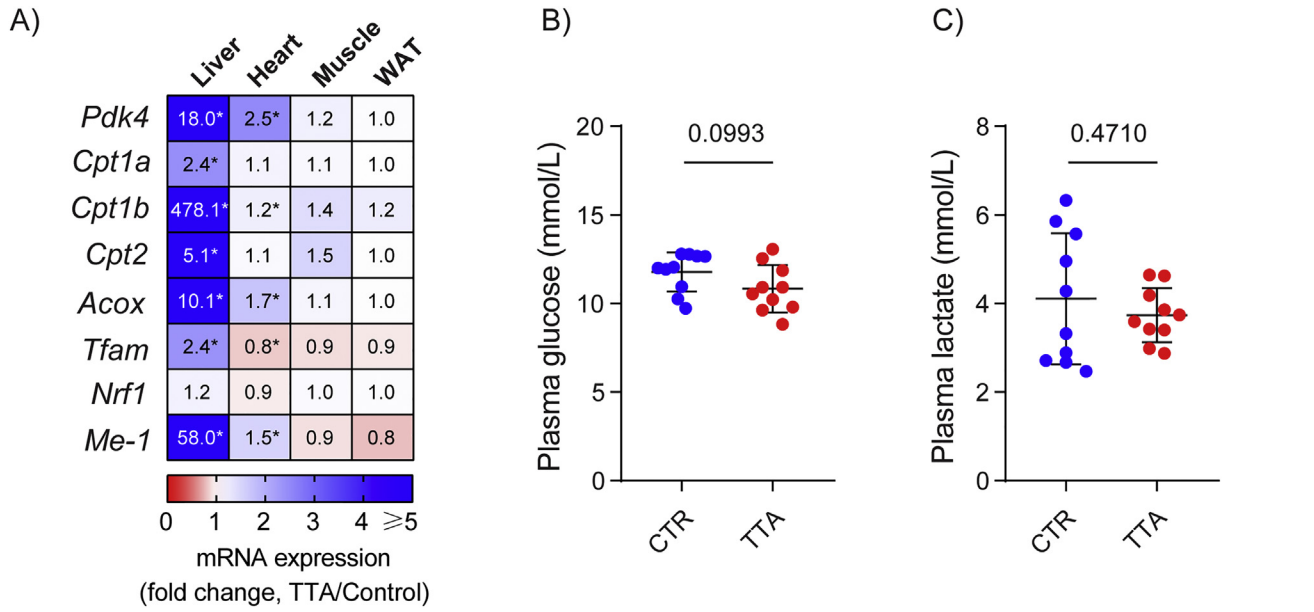

Fig. 1. *Pdk4* expression and metabolic adaptation in TTA-treated rats.
Rats were administered control (CTR) or TTA-supplemented diet for 50 weeks (Vigerust et al., 2012). (A) Gene expression in liver, heart, skeletal muscle and white adipose tissue (WAT) was measured using real time quantitative PCR. The heat map indicates mean expression level relative to control (ddCT method, detailed data in Supplementary Fig. S1). (B) Glucose and (C) lactate concentrations in plasma from the CTR and TTA fed rats. Each dot represent one animal and group mean ± SD (n = 8–10) is indicated. Statistical analysis was performed by t-test. *$p < .05$, p-values are shown in (B) and (C). TTA, tetradecylthioacetic acid.

Importantly, upregulation of fatty acid oxidation was accompanied by increased *Pdk4* expression, generally to a higher magnitude compared to other genes commonly used as indicators of mitochondrial fatty acid oxidation.

3.2. Fatty acid oxidation and PDK4 expression are strongly induced by PPARA-overexpression

As a proof of principle cell model where upregulation of fatty acid oxidation is expected, we investigated *PDK4* mRNA expression in MDA-MB-231 cells modified to overexpress *PPARA* (MDA-MB-231/PPARA, Fig. 2). Based on our previous experience with various cell models, the MDA-MB-231 line was chosen as the primary model due to its active oxidative metabolism, and the observation that these cells present a significant increase in fatty acid oxidation under relevant conditions. Several of the experiments were also repeated with HeLa cells, which we commonly find to display similar metabolic effects as MDA-MB-231, albeit often less pronounced.

The mRNA level of *PPARA* was 82.3 ± 14.4-fold higher in the MDA-MB-231/PPARA cells, compared to the parental cells. Noteworthy, this caused a 24.9 ± 1.8-fold increase in *PDK4* mRNA level, and upregulation of genes involved in fatty acid catabolism such as *ACOX* (51.0 ± 12.5), *CPT1A* (2.3 ± 0.1), *COX4I1* (1.9 ± 0.05) and *ME-1* (2.0 ± 0.03) (Fig. 2A). The expression of the mitochondrial transcription factor *TFAM* was slightly reduced (0.7 ± 0.04) in the MDA-MB-231/PPARA cells, suggesting that the increased expression of these mitochondrial enzymes was not linked to increased mitochondrial biogenesis.

To investigate if *PPARA* overexpression caused a metabolic fuel change, we measured glucose and fatty acid oxidation by trapping $^{14}CO_2$ produced under incubation with the respective radiolabeled substrates. Fatty acid oxidation was increased nearly three-fold in the MDA-MB-231/PPARA cells compared to the parental cells (Fig. 2B). In the same cells, glucose oxidation was reduced by 20%, when glucose was provided as the major substrate (Fig. 2C). These data support the notion that *PDK4* expression and fatty acid oxidation are co-regulated by PPARα, leading to an overall metabolic shift towards increased oxidation of fatty acid instead of glucose.

3.3. PDK4 overexpression leads to increased fatty acid oxidation

The increase in *PDK4* expression may occur as a parallel effect besides the stimulated fatty acid oxidation, or it may be a causative factor of the metabolic shift. To address this question, we investigated the effects of *PDK4* overexpression in MDA-MB-231 cells (i.e. MDA-MB-231/PDK4 cells). The levels of PDK4 mRNA and protein were low in the parental cells, and the increased amounts in the modified cells confirmed successful overexpression (Fig. 3A-B). Although the PDK4 antibody gave weak band intensity, the immunoblot showed increased level in PDK4-overexpressing cells (Fig. 3B). We then investigated if this leads to reduced pyruvate oxidation, which would be the expected consequence of PDK4-mediated inhibition of the PDH complex. Following incubation in high glucose environment (25 mM), pyruvate oxidation was 32% reduced in the MDA-MB-231/PDK4 cells (borderline statistical significance), compared to the parental cells (Fig. 3C). This activity was stimulated in both cell types when grown in low glucose compared to high glucose medium, but pyruvate oxidation remained lower in the MDA-MB-231/PDK4 compared to the parental cells. Noteworthy, fatty acid oxidation was 74% increased in *PDK4* overexpressing cells compared to parental cells when grown in 25 mM glucose, but the difference disappeared following growth in 1 mM glucose, primarily due to a significant increase in the parental cells (Fig. 3D). These data strongly support that there is a tight causative relationship between PDK4 and fatty acid oxidation. Apparently, *PDK4* overexpression lead to a shift towards fasting-type energy metabolism even in a high glucose environment. Hence, the differences between parental and *PDK4* overexpressing cells were smaller following growth in a low glucose environment, since this significantly enhanced fatty acid oxidation in the parental cells but not to the same extent in *PDK4*-overexpressing cells.

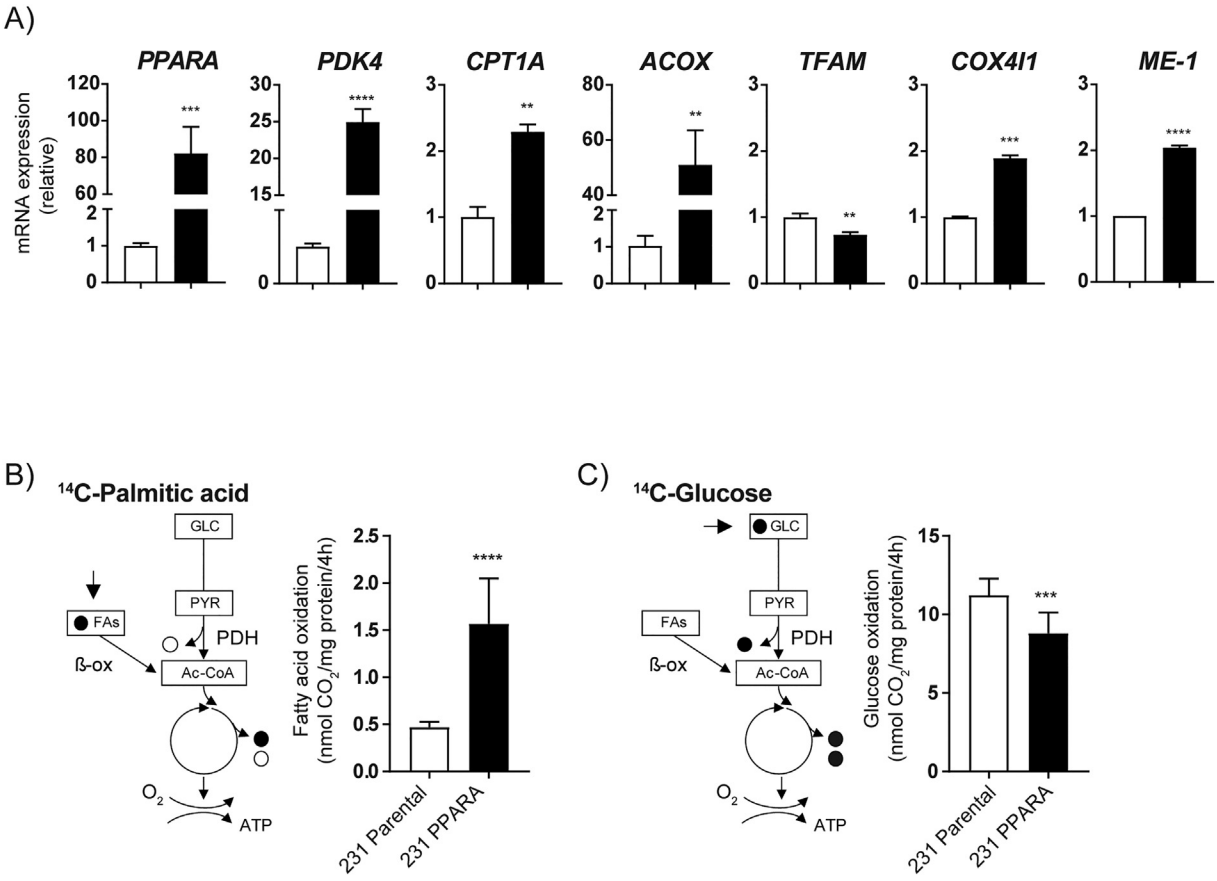

Fig. 2. Effect of *PPARA* overexpression on *PDK4* expression and fuel oxidation.
The effects of increased *PPARA* expression were investigated in MDA-MB-231 cells. The figure compares the unmodified (231 Parental) and *PPARA* overexpressing (231 PPARA) cells. (A) Expression of *PPARA*, *PDK4, CPT1A, ACOX, TFAM, COX4I1* and *ME-1*, measured using real time quantitative PCR. The diagrams show mRNA expression relative to the CTR group (ddCT method), as mean ± SD of triplicate measurements. (B) Fatty acid oxidation; $^{14}CO_2$-production during 4 h incubation with [1-^{14}C]palmitic acid (1 μCi/ml, 100 μM), in presence of L-carnitine (1 mM) and glucose (0.5 mM). (C) Glucose oxidation; $^{14}CO_2$-production during 4 h incubation with D-[^{14}C(U)]glucose (2 μCi/ml, 5 mM). The oxidation data are normalized to cell protein content (mg), and are displayed as mean ± SD of 4–8 replicates. The pathway illustrations show the carbon flux fueled by the ^{14}C-labeled substrates. The filled and open circles represent radiolabeled (filled, ^{14}C) and non-labeled (open) carbons, released as CO_2 under the respective conditions. The shown experiments are representative for three separate experiments. Statistical analysis was performed by *t*-test. $*p < .05$, $**p < .01$, $***p < .001$, $****p < .0001$.

3.4. Increased PDK4 expression reflects upregulated fatty acid oxidation under conditions of metabolic adaptation

In order to investigate the relationship between fatty acid oxidation and *PDK4* expression in different contexts of metabolic adaptation, we studied the effects of long-term (6 days) treatment with TTA and selective activators of AMPK (AICAR) and PPARα (WY 14,643) in MDA-MB-231 cells. The mRNA level of *CPT1A*, which often is used as an indicator of mitochondrial fatty acid oxidation, was lower after treatments with AICAR and WY 14,643, compared to control, but increased approximately two-fold in cultures treated with 30 μM or 60 μM TTA (Fig. 4A). The effect of TTA on *PDK4* expression was of significantly higher magnitude (7.3 ± 0.3 at 30 μM TTA, 12.2 ± 1.2 at 60 μM TTA) compared to *CPT1A*. AICAR treatment caused reduced *PDK4* expression, whereas WY 14,643 had no effect. None of the agents were found to induce the mRNA expression of the classical PPARα-target *ACOX* in these cells. Only AICAR induced the expression of *TFAM* (2.7 ± 0.1), suggesting that this treatment, in contrast to the others, causes activation of mitochondrial biogenesis. Replication of this experiment with Hela cells supported that TTA, but not AICAR and WY 14,643, caused moderate upregulation of *CPT1A* simultaneous with a strong induction of *PDK4* (Supplementary Fig. S2). HeLa cells tended to have a mild upregulation of *TFAM* and *ACOX* expression for all the treatments except for 60 μM TTA.

The highest concentration of TTA (60 μM) caused a 4-fold increase in basal fatty acid oxidation in MDA-MB-231 cells, and the effect was slightly less with the lower concentration (30 μM) (Fig. 4B). In our experience, functional changes of this magnitude in cell metabolism are rarely observed in living cell cultures. AICAR and WY 14,643 did not affect fatty acid oxidation in these cells. Additional measurements in presence of the mitochondrial uncoupler carbonyl cyanide 3-chlorophenylhydrazone (CCCP) showed that the maximal fatty acid oxidation capacity was approximately two-fold increased in the TTA-treated cells (for both TTA concentrations). Enhanced fatty acid oxidation in TTA-treated cells was not found to be accompanied by a reciprocal reduction in basal glucose oxidation, yet there was a moderate decrease in AICAR-treated cells (Fig. 4C). We then measured pyruvate oxidation in order to obtain a more direct assessment of mitochondrial oxidation, disconnected from the potential rate-limiting influence of glycolysis. Basal pyruvate oxidation tended to be reduced after treatment with 60 μM TTA, with as significant 30% reduction under uncoupling conditions (Fig. 4D). Similar effects were seen in HeLa cells after treatment with AICAR, WY 14,643 or TTA (Supplementary Fig. S2). In summary, metabolic adaptation involving induced fatty acid oxidation was accompanied by strongly increased *PDK4* mRNA expression in these cell models. This effect was observed after treatment with TTA known to regulate multiple energy-sensitive mechanisms, but not with selective activators of AMPK (AICAR) or PPARα (WY 14,643), under these

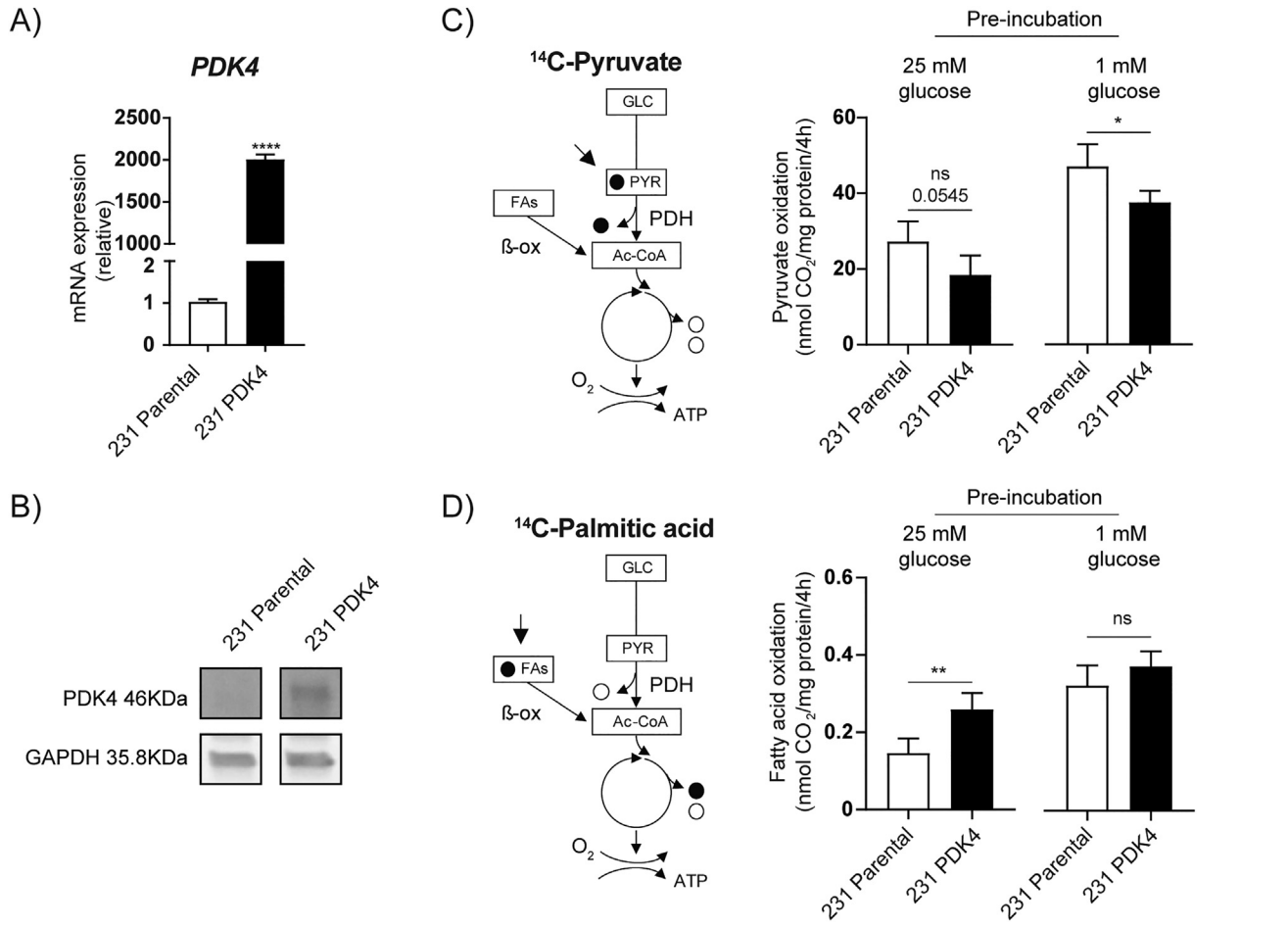

Fig. 3. Effect of *PDK4* overexpression in pyruvate and fatty acid oxidation.
The effects of *PDK4* overexpression were investigated in MDA-MB-231 cells. The figure compares the unmodified (231 Parental) and *PDK4* overexpressing (231 PDK4) cells. (A) Confirming overexpression of *PDK4* using real time quantitative PCR. The mRNA expression level is displayed relative to the 231 Parental cells (ddCT method) as mean ± SD of triplicate measurements, and is representative for two separate experiments. (B) Increased PDK4 protein expression was confirmed by Western blot analysis. (C-D) Pyruvate and fatty acid (palmitic acid) oxidation was measured following overnight pre-incubation in medium with 1 mM or 25 mM glucose. (C) Pyruvate oxidation; $^{14}CO_2$-production during 4 h incubation with [1-^{14}C]pyruvic acid (0.25 μCi/ml, 0.2 mM), in presence of glucose (0.5 mM). (D) Fatty acid oxidation; with [1-^{14}C]palmitic acid (1 μCi/ml, 100 μM), in presence of L-carnitine (1 mM) and glucose (0.5 mM). The oxidation data are normalized to cell protein content (mg) and are displayed as mean ± SD of 4–8 replicates, from one representative of three separate experiments. The pathway illustrations show carbon flux fueled by the ^{14}C-labeled substrates. The filled and open circles represent radiolabeled (filled, ^{14}C) and non-labeled (open) carbons released as CO_2 under the respective conditions. Statistical analysis was performed by *t*-test. *$p < .05$, **$p < .01$, ***$p < .001$, ****$p < .0001$.

experimental conditions.

A previously established genetic reporter strategy was utilized to further evaluate the potential role of mitochondrial biogenesis under these conditions (Hodneland Nilsson et al., 2015). The reporter construct consists of a gene for mitochondrial GFP under the control of a responsive element of NRF1, which is a central nuclear transcription factor controlling expression of mitochondrial proteins. Single cell analysis was performed by flow cytometry in HeLa and MDA-MB-231 cells containing the reporter construct, following treatments with AICAR, WY 14,643 or TTA (Fig. 4E). Only AICAR was found to have a significant effect on mitochondrial biogenesis in HeLa cells, and this agreed with the findings in MDA-MB-231 cells (borderline statistical significance). This effect of AICAR was also previously observed in HeLa cells (Hodneland Nilsson et al., 2015). Both the genetic reporter results and the *TFAM* expression data indicated that the fuel shift from glucose to fatty acids occurs without simultaneous induction of mitochondrial biogenesis in these cell types. Western blot analysis supported that PDK4 protein abundance was increased following treatment with TTA, but not WY 14,643, in HeLa cells (Fig. 4F).

3.5. Effects of metabolic adaptation on mitochondrial respiration and glycolysis

To investigate if increased fatty acid oxidation was associated with changes in mitochondrial respiration, we measured oxygen consumption rate (OCR) in MDA-MB-231 cells after long-term (6 days) treatment with AICAR, WY 14,643 or TTA, and upon overexpression of *PPARA* (Fig. 5). Following measurement of the basal respiratory rate, we assessed descriptors of mitochondrial function through sequential additions of pharmacological modulators. Leak respiration rate was obtained after addition of oligomycin (ATP synthase inhibitor), and subsequently CCCP was administered to measure uncoupled respiratory capacity. Rotenone (respiratory complex I inhibitor) was then added, followed by antimycin A (respiratory complex III inhibitor) to assess non-mitochondrial activity (residual oxygen consumption, background activity). Interestingly, the basal respiratory rates were similar among the different conditions of metabolic adaptation (AICAR, WY 14,643, TTA and *PPARA* overexpression), and compared to respective controls (untreated and DMSO (vehicle)), with a minor increase in cultures treated with WY 14,643 and 60 μM TTA. Leak respiration was increased 2–3-fold in the TTA treated cultures compared to control (DMSO),

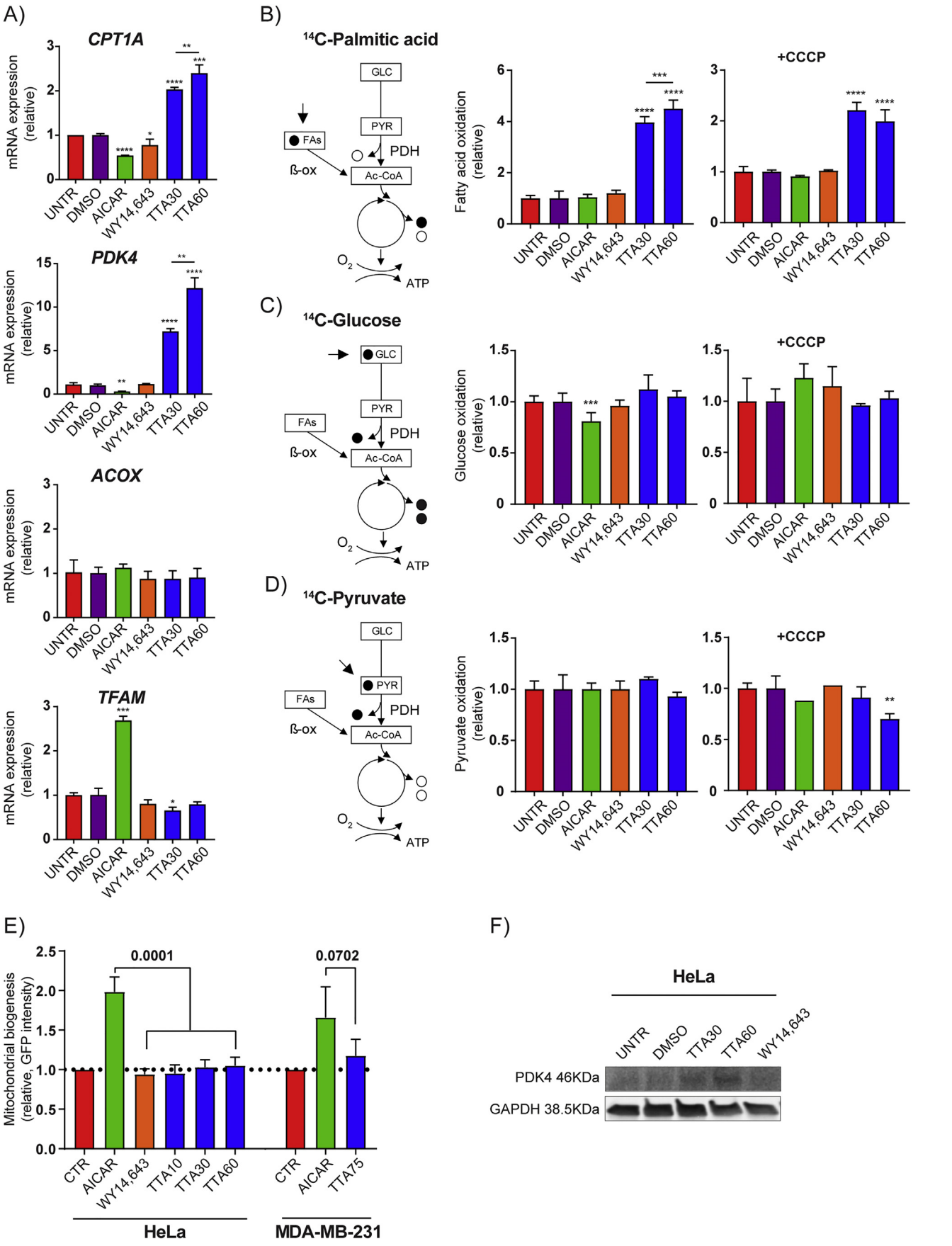

(caption on next page)

Fig. 4. *PDK4* expression and fatty acid oxidation in contexts of metabolic adaptation.
MDA-MB-231 were treated for 6 days with AICAR (0.5 mM), WY 14,643 (10 μM) or TTA (30 μM or 60 μM). Control cultures were untreated (UNTR, for AICAR) or DMSO-treated (DMSO, for WY 14,643 and TTA). (A) Real time quantitative PCR analysis of *TFAM*, *ACOX*, *CPT1A* and *PDK4*. The diagrams show mRNA expression relative to the control group (ddCT method), as mean ± SD of triplicate measurements. (B-D) Substrate oxidation was assessed by measuring $^{14}CO_2$-production during 4 h incubation with the respective radiolabeled substrate, in the absence and presence of an uncoupler (CCCP). (B) Fatty acid oxidation; with [1-^{14}C]palmitic acid (1 μCi/ml, 100 μM), in presence of L-carnitine (1 mM) and glucose (0.5 mM). (C) Glucose oxidation; with D-[^{14}C(U)]glucose (2 μCi/ml, 5 mM). (D) Pyruvate oxidation; with [1-^{14}C]pyruvic acid (0.25 μCi/ml, 2 mM). CCCP concentrations were 1 μM for glucose and pyruvate oxidation, and 3 μM for palmitic acid oxidation (higher due to the increased BSA concentration). The oxidation data are normalized to cell protein content (mg) and shown as mean ± SD of 4–8 replicates. The pathway illustrations show the carbon flux fueled by the ^{14}C-labeled substrates. The filled and open circles represent radiolabeled (filled, ^{14}C) and non-labeled (open) carbons, released as CO_2 under the respective conditions. (E) Measurement of mitochondrial biogenesis using a GFP-based reporter construct in HeLa and MDA-MB-231 cells. The reporter cells were treated before mitoGFP was detected by flow cytometry (10,000 cells per sample). (F) Western blot analysis of PDK4 in HeLa cells treated for 6 days with TTA (30 μM or 60 μM) or WY 14,643 (10 μM). All diagrams display representative data as, mean ± SD, for three separate experiments. Statistical analysis was performed by *t*-test. *$p < .05$, **$p < .01$, ***$p < .001$, ****$p < .0001$.

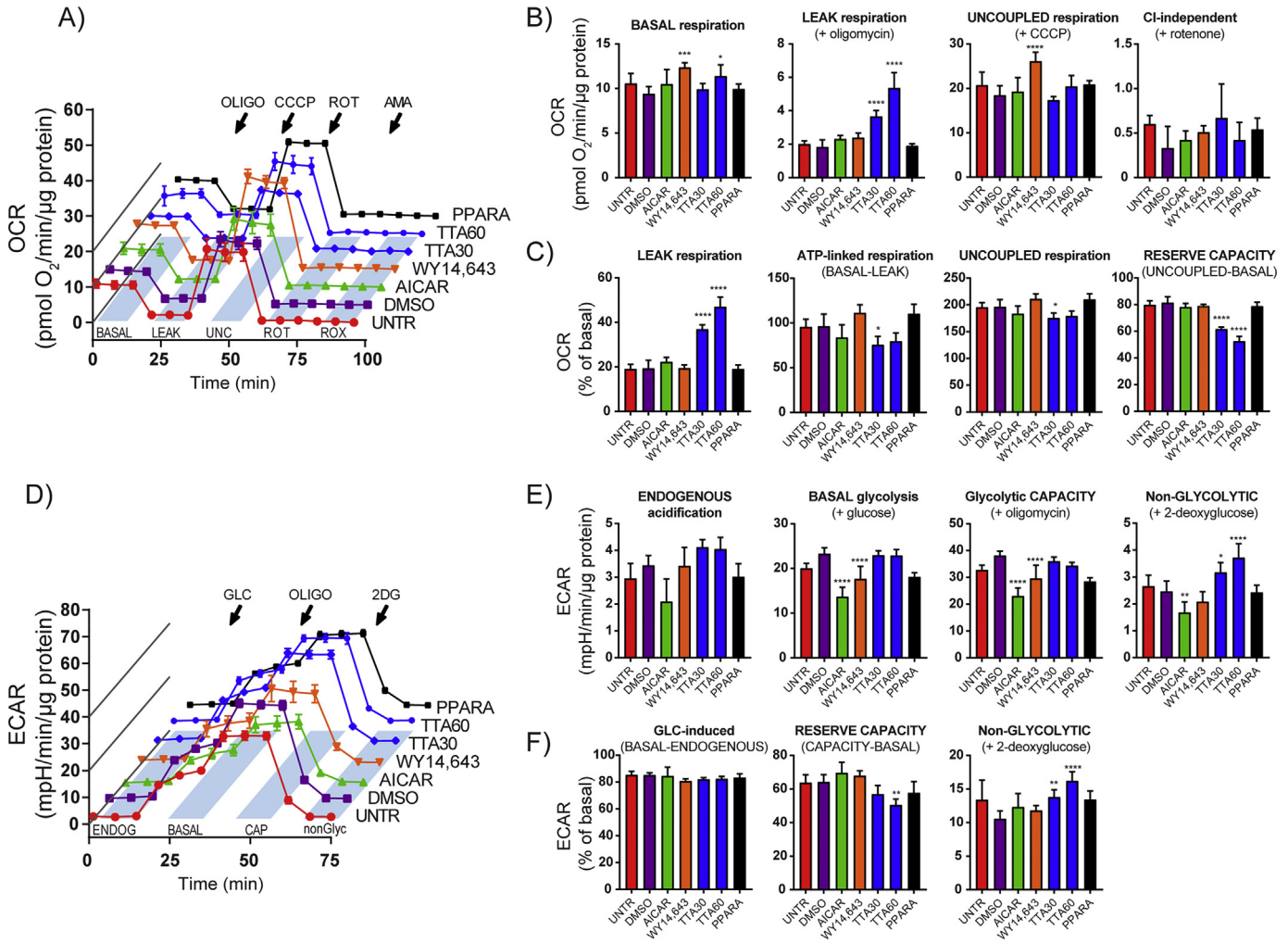

Fig. 5. Analysis of mitochondrial respiration and glycolysis.
Oxygen consumption rate (OCR) and extracellular acidification rates (ECAR) were measured in MDA-MB-231 cells after 6 days treatment with AICAR (0.5 mM), WY 14,643 (10 μM) and TTA (30 μM or 60 μM), and in cells overexpressing *PPARA*. Control cultures were untreated (UNTR, for AICAR and PPARA) or DMSO-treated (DMSO, for WY 14,643 and TTA) cells. (A) Representative traces of OCR (pmol O_2/min/μg protein). Following measurement of basal respiration (BASAL), specific modulators were added as indicated: 3 μM oligomycin to obtain leak respiration (LEAK), 1 μM CCCP to access uncoupled respiration (UNC), 1 μM rotenone to measure rotenone-resistant respiration (ROT) and 1 μM antimycin A to measure residual oxygen consumption (ROX). (B) Data extracted from the analyses in A, after subtraction of non-mitochondrial activity (ROX). (C) Analysis of functional integrity of mitochondria. Rates of interest calculated as % of basal OCR. (D) Representative traces of ECAR (mpH/min/μg protein). The specific modulators were added following measurement of endogenous activity (ENDOG), as indicated: 10 mM glucose (GLC) to obtain basal glycolysis (BASAL), 3 μM oligomycin to assess glycolytic capacity (CAP) and 100 mM 2-deoxyglucose (2DG) to measure non-glycolytic activity (non-Glyc). (E) Data extracted from the analyses in D. (F) Analysis of glycolytic function. Rates of interest calculated as % of basal ECAR. Data are displayed as mean ± SD of 6–8 replicates, from one representative of three separate experiments Statistical analysis was performed by ANOVA. *$p < .05$, **$p < .01$, ***$p < .001$, ****$p < .0001$.

apparently in a concentration-dependent manner. The uncoupled respiratory capacity was not significantly affected by AICAR, TTA or *PPARA*-overexpression, however, WY 14,643 caused approximately 20% increase compared to the control (DMSO) (Fig. 5B). Calculating these data as percentage of the basal respiratory rate (Fig. 5C) revealed that TTA significantly increased the fraction of oxygen consumption associated with leak respiration, and therefore caused a congruent decrease in ATP-linked respiration. The effects of the treatments on the relative respiratory capacity (uncoupled) were generally negligible, while TTA significantly reduced the reserve capacity. The findings were reproduced in HeLa cells (Supplementary Fig. S3). In summary, the highly increased fatty acid oxidation rate observed after treatment with TTA and upon overexpression of *PPARA* was not associated with major changes in basal mitochondrial respiration. However, TTA led to effects consistent with mild uncoupling, which may represent an additional mechanism contributing to metabolic adaptations.

Analysis of glycolytic function was performed by monitoring extracellular acidification rate (ECAR) following sequential additions of glucose to obtain basal respiratory rate, oligomycin to measure glycolytic capacity, and 2-deoxyglucose to determine non-glycolytic activity (Fig. 5D). There was a general reduction in normalized ECAR after treatment with AICAR and WY 14,643 in MDA-MB-231 cells (Fig. 5E), but upon additions of glucose and upon addition of oligomycin, the relative rates were similar to control (Fig. 5F), suggesting that glycolysis was modulated as normal under these conditions. No change in glycolytic activity was found in *PPARA*-overexpressing cells, compared to control cells. TTA-treated cells were also similar to control, but had a relatively high non-glycolytic acidifying component, displayed both before addition of glucose and after addition of 2-deoxyglucose. The TTA-treated cells tended to have slightly reduced reserve glycolytic capacity, and this was statistically significant in the cultures treated with 60 μM TTA (Fig. 5F). Similar findings were obtained in HeLa cell cultures, where TTA also caused a statistically significant increase in normalized basal glycolysis (Supplementary Fig. S3). In summary, the effects of metabolic modulators on glycolysis did not demonstrate a strong correlation with the changes in fatty acid oxidation under these conditions.

3.6. Mild uncoupling may contribute to increased fatty acid oxidation upon TTA-treatment

Based on the obtained data suggesting an uncoupling effect of TTA on mitochondrial respiration, we designed an experiment to investigate if TTA may mediate such effects through an acute mechanism. TTA was compared with palmitic acid, a normal saturated fatty acid, when added at different concentrations to MDA-MB-231 cells immediately before OCR analysis (Fig. 6A-B). Acute uncoupling activity could then be detected as an increase in leak respiration after addition of oligomycin. The data clearly demonstrated that TTA, but not palmitic acid, caused a concentration-dependent increase in leak respiration (Fig. 6C). Both TTA and palmitic acid caused a minor concentration-dependent decrease in uncoupled respiration after addition of CCCP (Fig. 6D). The uncoupling property of TTA was found to be relatively mild, as the highest concentration of 200 μM, which exceeds the normally tolerable concentration for cell survival, caused approximately 30% uncoupling compared to full uncoupling mediated by 1 μM CCCP (Fig. 6E). These findings were also reproduced in HeLa cells (Supplementary Fig. S4). Our data suggest mild uncoupling as a new mechanism of TTA, which induces an additional energy stress likely to influence and accentuate effects on nutrient-sensitive fueling pathways to support energy homeostasis. Such a mechanism may explain the effects related to the changed energy state previously observed in rat liver (Grav et al., 2003).

3.7. PDK4 expression reports synergistic effects of TTA and rapamycin on fatty acid oxidation

Rapamycin, an inhibitor of mTOR, has previously been found to increase fatty acid oxidation (Sipula et al., 2006). Further, studies in rat hepatocytes have linked the effects of TTA to regulation of mTOR (Hagland et al., 2013). To investigate if mTOR inhibition influences TTA-mediated metabolic adaptation, we treated MDA-MB-231 with TTA and rapamycin, separately and in combination. Rapamycin alone did not affect mRNA expression of *CPT1A* and *PDK4*. In combination with TTA, however, the levels of both these mRNAs were significantly higher than in cells treated with TTA alone (Fig. 7A-B). Exactly the same pattern was seen on rates of fatty acid oxidation, both under basal and uncoupled conditions (CCCP) (Fig. 7C). Further, we performed correlation analysis of *PDK4* and *CPT1A* expression relative to fatty acid oxidation, with data from different conditions of metabolic adaptation (Fig. 7D). Expression of *PDK4* and *CPT1A* was found to correlate strongly with each other, and with fatty acid oxidation activity. These data support a tight regulatory and functional relationship between *PDK4* expression and fatty acid oxidation in different metabolic contexts. An advantage of using *PDK4*, above *CPT1A*, as an indicator of fatty acid oxidation would be the significantly higher magnitude of induction, and therefore a larger dynamic range and higher sensitivity.

4. Discussion

This study shows that upregulated *PDK4* mRNA expression is strongly associated with increased activity of mitochondrial fatty acid oxidation in metabolically adapted cells and rat tissues. Overall, we found good correlation between the relative magnitude of *PDK4* upregulation and the accompanying increase in fatty acid oxidation. Based on these findings, we suggest that *PDK4* mRNA expression may be used as a sensitive surrogate marker for changes in mitochondrial fatty acid oxidation when investigating (pato)physiological adaptations of energy metabolism.

The activity of mitochondrial fatty acid oxidation is influenced by many factors, including diet, physical activity, toxic exposure, epigenetics and mutations. An unhealthy impact on fatty acid oxidation could lead to suboptimal energy balance, energy deficiency, excessive lipid storage and metabolic stresses, which ultimately contribute to pathogenesis both at an organ and systemic level (Adeva-Andany et al., 2018). On the other hand, metabolic adaptations may have positive impact, for instance in response to endurance training which increases the capacity of mitochondrial fatty acid oxidation to accommodate the elevated demands of energy (ATP) (Booth et al., 2015). In the laboratory, mitochondrial fatty acid oxidation may be assessed by measuring the products formed when radiolabeled fatty acid substrates are provided to intact cells or fresh preparations (extracts, homogenates) of cell cultures or tissues (e.g. (Wensaas et al., 2007)). However, such methods are often inaccessible, or incompatible with regards to the available sample material. Measurement of surrogate markers, such as mRNA expression of relevant genes, may therefore represent an attractive strategy to study regulatory effects on fatty acid oxidation. As far as we know, there is no consensus to which gene targets that are optimal for serving as expression reporters of a metabolic shift involving increase in fatty acid oxidation. As for enzymes of the fatty acid oxidation machinery, the changes in mRNA expression are often found subtle and with complex cell-type specific regulation. Therefore, we investigated *PDK4* expression as a possible candidate for such purpose, under conditions of metabolic adaptation driven by different regulatory programs involving AMPK, PPARs and mTOR, which are relevant for mechanisms of exercise, starving, obesity and contexts of defective metabolism.

In rats that were treated with TTA for 50 weeks, we found significantly increased expression of *Pdk4* particularly in liver, and to some extent in heart, but not in skeletal muscle and white adipose tissue

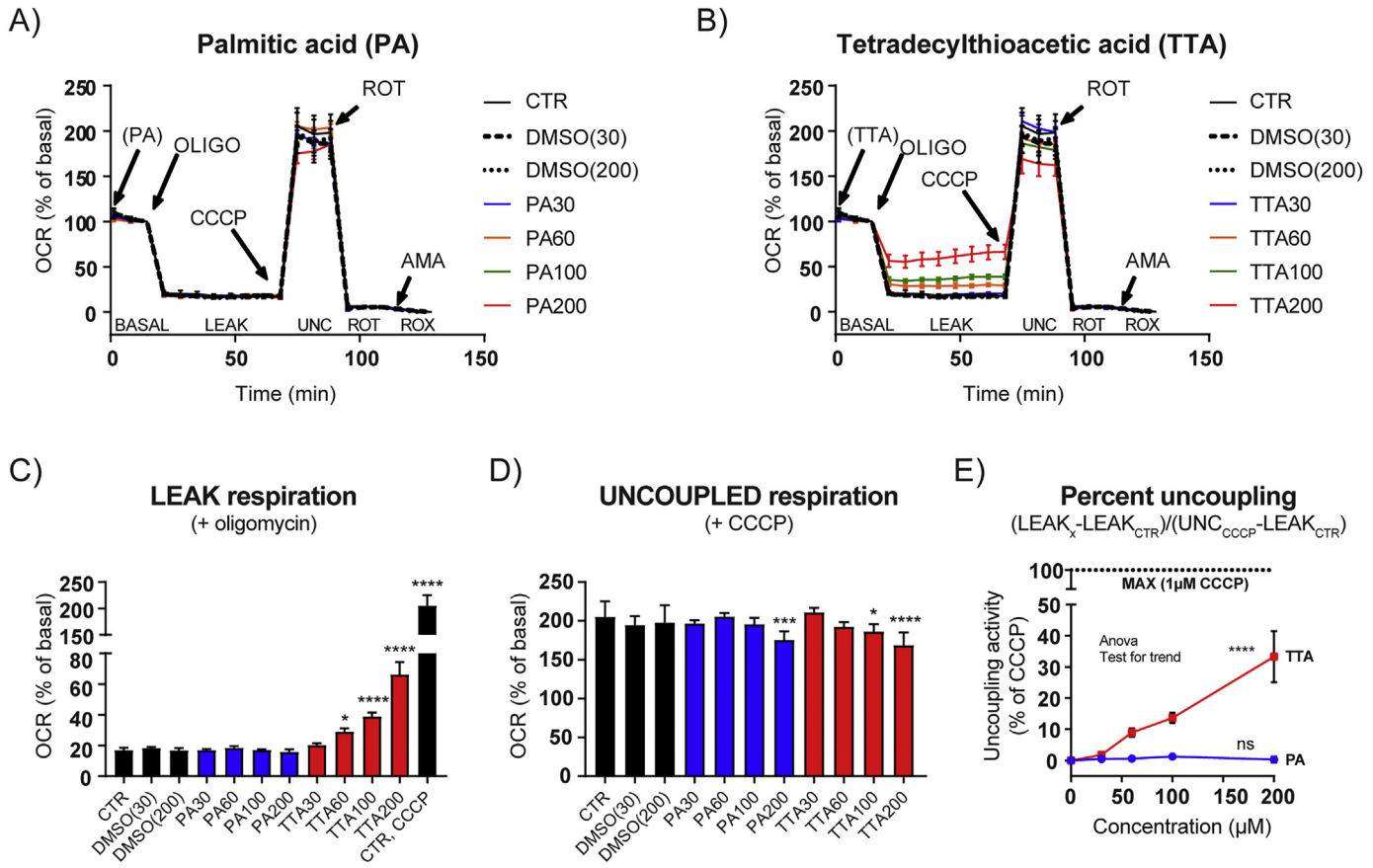

Fig. 6. TTA exerts mild uncoupling activity.

Oxygen consumption rate (OCR) was measured in MDA-MB-231 cells immediately after administration palmitic acid (PA) or tetradecylthioacetic acid (TTA), at concentrations of 30–200 μM. (A-B) Representative traces of OCR as % of initial rate (BASAL), in presence of PA or TTA. Specific modulators were added as indicated: 3 μM oligomycin to obtain leak respiration (LEAK), 1 μM CCCP to access uncoupled respiration (UNC), 1 μM rotenone to measure rotenone-resistant respiration (ROT) and 1 μM antimycin A to measure residual oxygen consumption (ROX). (C) LEAK respiration and (D) UNCOUPLED respiration shown as % of basal OCR. (E) Uncoupling activity mediated by PA and TTA, compared to complete uncoupler, CCCP (100%). The agent-induced LEAK rate (i.e. $LEAK_X$ - $LEAK_{CTR}$) was calculated relative to the CCCP-induced LEAK rate (i.e. UNC_{CCCP}-$LEAK_{CTR}$). Data are displayed as mean ± SD of 6–8 replicates, from one representative of three separate experiments. Statistical analysis was performed by ANOVA. *$p < .05$, **$p < .01$, ***$p < .001$, ****$p < .0001$.

(WAT). This parallels well with increased rates of mitochondrial fatty acid oxidation especially in liver, and also in heart tissue, of TTA-treated rats (Berge et al., 2005; Oie et al., 2013). In addition, we found a pronounced increase in the muscle isoform *Cpt1b* in liver, yet only a minor increase in heart, and no detectable effect in muscle and WAT. TTA also caused significantly increased *Me-1* expression in rat liver, supporting that strengthened TCA anaplerotism contributes to the adaptation of high mitochondrial fatty acid oxidation rates (Gibala et al., 2000; Carley et al., 2015). These data underscore the importance of context- and tissue-specific influences on gene regulation associated with the fatty acid oxidation machinery. Interestingly, PDK4 upregulation was consistently presented under conditions of increased fatty acid oxidation in our studies, both in vivo and in vitro.

In cultured MDA-MB-231 cells, we found highly increased *PDK4* expression accompanying enhanced mitochondrial fatty acid oxidation upon *PPARA*-overexpression and after long-term treatment with TTA. Congruently, *PDK4*-overexpression caused reduced pyruvate oxidation simultaneously with increased fatty acid oxidation when the cells were grown in high glucose. When transferred to low glucose conditions, fatty acid oxidation in the parental cells increased to the same level as the *PDK4*-overexpressing cells. This supports the theory that increased *PDK4* expression contributes to fasting/starving-type metabolism with stimulated fatty acid oxidation (Wu et al., 2000), and our findings suggest that this program is constitutively active in the *PDK4*–overexpressing cells. Hence, there is strong evidence for a tight regulatory and functional relationship between *PDK4* and the fatty acid oxidation pathway. Direct activation of PPARα with WY-14,643 had no effect on fatty acid oxidation in MDA-MB-231 cells, possibly due to a low endogenous amount of this transcription factor, since overexpression caused classical effects on cellular gene expression and metabolism. The AMPK activator AICAR induced *TFAM* expression, suggestive of increased mitochondrial biogenesis as previously observed in HeLa cells (Hodneland Nilsson et al., 2015); however, there was no effect on mitochondrial fatty acid oxidation. On the contrary, AICAR had a suppressive effect on *CPT1A* and *PDK4* expression. This is compatible with previous findings in rat adipose tissue (Wan et al., 2010), but not in skeletal muscle (Merrill et al., 1997). Interestingly, in addition to the known function as panPPAR activator, TTA was found to act directly as a mild mitochondrial uncoupler, which may contribute to the changed energy state previously observed in rat liver (Grav et al., 2003). In that study, reduced mitochondrial membrane potential was found in rat liver after treatment with TTA, however, it remained unclear if this could be a direct or indirect mechanism. Due to the acute effects in our present cell culture study, it seems likely that TTA has a direct uncoupling effect on the mitochondrial inner membrane.

Inhibition of mTOR by rapamycin did not induce fatty acid oxidation or *PDK4* expression in MDA-MB-231 cells, but it accentuated the effects of TTA, suggesting that mTOR can act together with other pathways of metabolic adaptation in a context-dependent manner. In support, mTOR has been found to be regulated by the level of PDK4 in

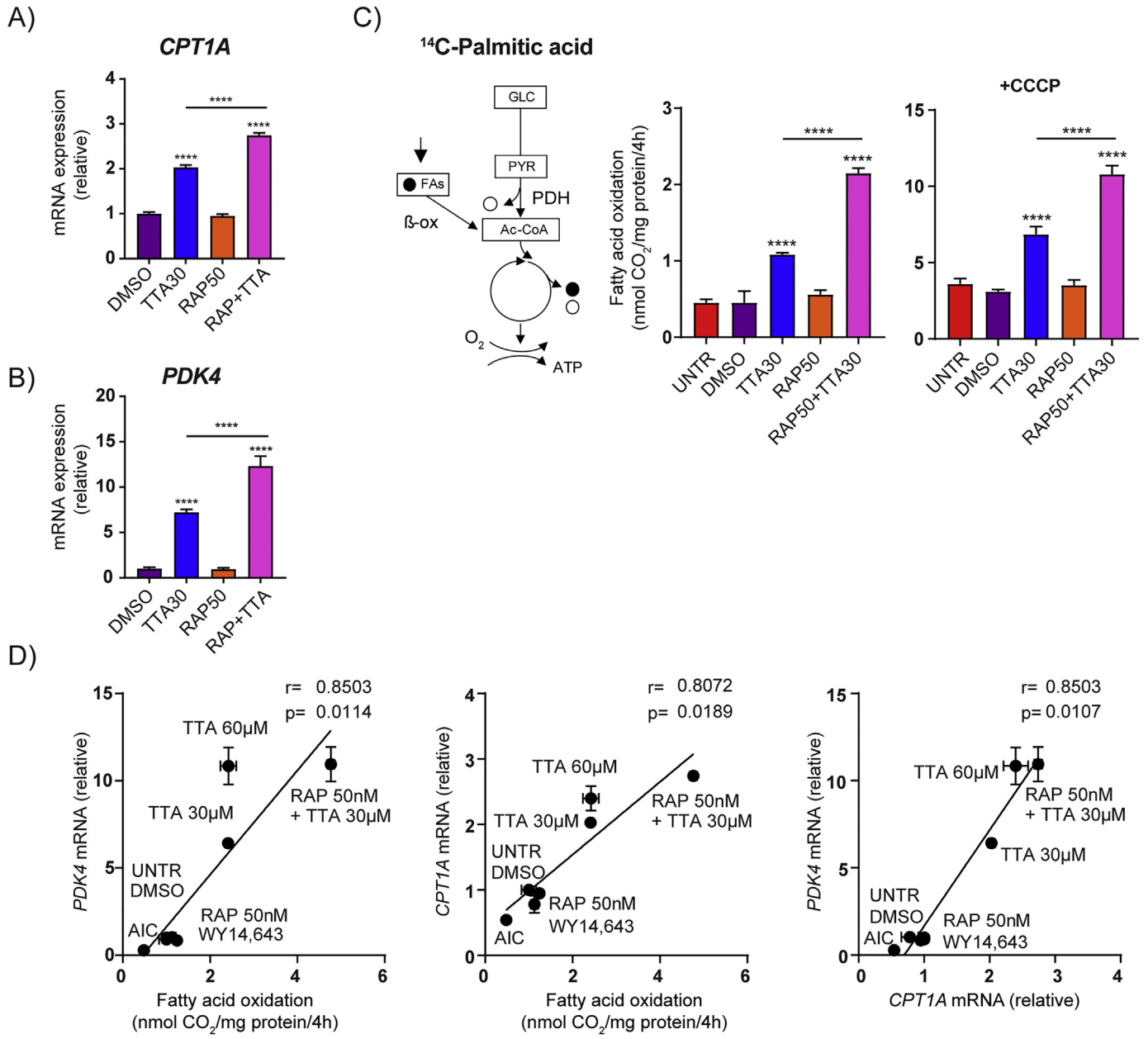

Fig. 7. Synergistic effects of TTA and rapamycin on fatty acid oxidation.
MDA-MB-231 were treated for 6 days with TTA (30 μM) or rapamycin (50 nM, RAP), separately and in combination. (A) *CPT1A* and (B) *PDK4* expression was measured using real time quantitative PCR as mean ± SD of triplicate measurements. (C) Fatty acid oxidation was assessed by measuring $^{14}CO_2$-production during 4 h incubation with [1-^{14}C]palmitic acid (1 μCi/ml, 100 μM) in presence of L-carnitine (1 mM) and glucose (0.5 mM), with and without an uncoupler (3 μM CCCP). The oxidation data are normalized to cell protein content (mg). The pathway illustrations show the carbon flux fueled by the ^{14}C-labeled palmitic acid. The filled and open circles represent radiolabeled (filled, ^{14}C) and non-labeled (open) carbons, released as CO_2 under the respective conditions. (D) Correlation analysis (Spearman) of data obtained from multiple conditions of metabolic adaptation. *PDK4* mRNA expression was analyzed relative to fatty acid oxidation and *CPT1A* expression. The oxidation data are shown as mean ± SD of 4–8 replicates, from one representative for three separate experiments. Statistical comparisons was performed by ANOVA. *p < .05, **p < .01, ***p < .001, ****p < .0001.

cultured cells (Liu et al., 2014). In separate experiments, we found the effects in HeLa cells to be similar to the observations in MDA-MB-231 cells.

A rather striking observation was the minor changes regarding mitochondrial respiration and lactate production under basal cell culture assay conditions, despite the pronounced changes in metabolic fuel utilization indicated by increased fatty acid oxidation. This suggests that the increase in fatty acid oxidation did not change the activity balance between mitochondrial respiration and glycolysis, but rather a change in substrate preference serving to maintain the supply of acetyl-CoA for the TCA cycle. This type of cellular metabolic adaptation is likely to affect properties of metabolic flexibility and associated stress mechanisms, and therefore the susceptibility for changes in nutrient supply. The present study primarily investigated metabolic effects under standard cell culture conditions, which includes high glucose concentration (normally 25 mM in DMEM), and favorable effects on glycolysis are expected to occur under such conditions. The dependency on mitochondrial oxidative metabolism following relevant adaptations of fuel utilization may be addressed further e.g. by reducing the amount of glucose, or replacing glucose with galactose in the culture medium (Arroyo et al., 2016).

Systemic and cellular nutrient-sensitive mechanisms in the body

interact to mediate adaptations to changed metabolic needs or conditions (e.g. due to activity or diet). For instance, increased release of free fatty acids from adipose tissue under fasting would be expected to influence metabolism in relevant tissues, partly through ligand activation of PPARs. The effects of such events will vary depending on tissue and cell type. Therefore, it was interesting to find that increased *PDK4* expression was a rather consistent sign of increased fatty acid oxidation throughout this study. Measuring *PDK4* may be relevant in clinical investigations, as exemplified by the finding that upregulated *PDK4* expression in blood cells was associated with impaired PDH function in ME/CFS patients (Fluge et al., 2016), which may involve adaptations of fatty acid oxidation (Naviaux et al., 2016; Germain et al., 2017). Furthermore, diurnal variation in *PDK4* expression in blood cells was recently reported to be associated with plasma free fatty acid levels, supporting that this mirrors an important aspect of metabolic fuel switching (Yamaguchi et al., 2018). Hence, based on these findings, and supported by the current literature, upregulated *PDK4* expression appears as a sensitive marker for metabolic adaptations involving increased rates of mitochondrial fatty acid oxidation.

Acknowledgements

We are grateful to Sissel Vik Berge and Endre Stigen for their excellent technical assistance, and to Stein-Rune Lindhom for the custom made equipment for $^{14}CO_2$-trapping. Flow cytometry was performed using the infrastructure of The Bergen Flow Cytometry Core Facility, Department of Clinical Science, University of Bergen, Norway. The work was funded by grants from the Research Council of Norway (272680), and the Kavli Trust, Norway.

Declaration of Competing Interest

The authors declare that they have no conflicts of interest with the contents of this article.

Appendix A. Supplementary data

Supplementary data to this article can be found online at https://doi.org/10.1016/j.mito.2019.07.009.

References

Adeva-Andany, M.M., Carneiro-Freire, N., Seco-Filgueira, M., Fernandez-Fernandez, C., Mourino-Bayolo, D., 2019. Mitochondrial beta-oxidation of saturated fatty acids in humans. Mitochondrion 46, 73–90.

Arroyo, J.D., Jourdain, A.A., Calvo, S.E., Ballarano, C.A., Doench, J.G., Root, D.E., Mootha, V.K., 2016. A genome-wide CRISPR death screen identifies genes essential for oxidative phosphorylation. Cell Metab. 24, 875–885.

Badin, P.M., Loubiere, C., Coonen, M., Louche, K., Tavernier, G., Bourlier, V., Mairal, A., Rustan, A.C., Smith, S.R., Langin, D., Moro, C., 2012. Regulation of skeletal muscle lipolysis and oxidative metabolism by the co-lipase CGI-58. J. Lipid Res. 53, 839–848.

Berge, R.K., Tronstad, K.J., Berge, K., Rost, T.H., Wergedahl, H., Gudbrandsen, O.A., Skorve, J., 2005. The metabolic syndrome and the hepatic fatty acid drainage hypothesis. Biochimie 87, 15–20.

Booth, F.W., Ruegsegger, G.N., Toedebusch, R.G., Yan, Z., 2015. Endurance exercise and the regulation of skeletal muscle metabolism. Prog. Mol. Biol. Transl. Sci. 135, 129–151.

Cadoudal, T., Distel, E., Durant, S., Fouque, F., Blouin, J.M., Collinet, M., Bortoli, S., Forest, C., Benelli, C., 2008. Pyruvate dehydrogenase kinase 4: regulation by thiazolidinediones and implication in glyceroneogenesis in adipose tissue. Diabetes 57, 2272–2279.

Carley, A.N., Taglieri, D.M., Bi, J., Solaro, R.J., Lewandowski, E.D., 2015. Metabolic efficiency promotes protection from pressure overload in hearts expressing slow skeletal troponin I. Circ. Heart Fail. 8, 119–127.

Desvergne, B., Michalik, L., Wahli, W., 2006. Transcriptional regulation of metabolism. Physiol. Rev. 86, 465–514.

Dyrstad, S.E., Tusubira, D., Knappskog, S., Tronstad, K.J., Rosland, G.V., 2018. Introducing nano-scale quantitative polymerase chain reaction. Biochem. Biophys. Res. Commun. 506, 923–926.

Feng, Y.Z., Nikolic, N., Bakke, S.S., Boekschoten, M.V., Kersten, S., Kase, E.T., Rustan, A.C., Thoresen, G.H., 2014. PPARdelta activation in human myotubes increases mitochondrial fatty acid oxidative capacity and reduces glucose utilization by a switch in substrate preference. Arch. Physiol. Biochem. 120, 12–21.

Finck, B.N., Lehman, J.J., Leone, T.C., Welch, M.J., Bennett, M.J., Kovacs, A., Han, X., Gross, R.W., Kozak, R., Lopaschuk, G.D., Kelly, D.P., 2002. The cardiac phenotype induced by PPARalpha overexpression mimics that caused by diabetes mellitus. J. Clin. Invest. 109, 121–130.

Fluge, O., Mella, O., Bruland, O., Risa, K., Dyrstad, S.E., Alme, K., Rekeland, I.G., Sapkota, D., Rosland, G.V., Fossa, A., Ktoridou-Valen, I., Lunde, S., Sorland, K., Lien, K., Herder, I., Thurmer, H., Gotaas, M.E., Baranowska, K.A., Bohnen, L.M., Schafer, C., McCann, A., Sommerfelt, K., Helgeland, L., Ueland, P.M., Dahl, O., Tronstad, K.J., 2016. Metabolic profiling indicates impaired pyruvate dehydrogenase function in myalgic encephalopathy/chronic fatigue syndrome. JCI Insight 1, e89376.

Fukawa, T., Yan-Jiang, B.C., Min-Wen, J.C., Jun-Hao, E.T., Huang, D., Qian, C.N., Ong, P., Li, Z., Chen, S., Mak, S.Y., Lim, W.J., Kanayama, H.O., Mohan, R.E., Wang, R.R., Lai, J.H., Chua, C., Ong, H.S., Tan, K.K., Ho, Y.S., Tan, I.B., Teh, B.T., Shyh-Chang, N., 2016. Excessive fatty acid oxidation induces muscle atrophy in cancer cachexia. Nat. Med. 22, 666–671.

Galgani, J.E., Moro, C., Ravussin, E., 2008. Metabolic flexibility and insulin resistance. Am. J. Physiol. Endocrinol. Metab. 295, E1009–E1017.

Germain, A., Ruppert, D., Levine, S.M., Hanson, M.R., 2017. Metabolic profiling of a myalgic encephalomyelitis/chronic fatigue syndrome discovery cohort reveals disturbances in fatty acid and lipid metabolism. Mol. BioSyst. 13, 371–379.

Gibala, M.J., Young, M.E., Taegtmeyer, H., 2000. Anaplerosis of the citric acid cycle: role in energy metabolism of heart and skeletal muscle. Acta Physiol. Scand. 168, 657–665.

Grav, H.J., Tronstad, K.J., Gudbrandsen, O.A., Berge, K., Fladmark, K.E., Martinsen, T.C., Waldum, H., Wergedahl, H., Berge, R.K., 2003. Changed energy state and increased mitochondrial beta-oxidation rate in liver of rats associated with lowered proton electrochemical potential and stimulated uncoupling protein 2 (UCP-2) expression: evidence for peroxisome proliferator-activated receptor-alpha independent induction of UCP-2 expression. J. Biol. Chem. 278, 30525–30533.

Hagland, H.R., Nilsson, L.I., Burri, L., Nikolaisen, J., Berge, R.K., Tronstad, K.J., 2013. Induction of mitochondrial biogenesis and respiration is associated with mTOR regulation in hepatocytes of rats treated with the pan-PPAR activator tetradecylthioacetic acid (TTA). Biochem. Biophys. Res. Commun. 430, 573–578.

Hodneland Nilsson, L.I., Nitschke Pettersen, I.K., Nikolaisen, J., Micklem, D., Avsnes Dale, H., Vatne Rosland, G., Lorens, J., Tronstad, K.J., 2015. A new live-cell reporter strategy to simultaneously monitor mitochondrial biogenesis and morphology. Sci. Rep. 5, 17217.

Holness, M.J., Sugden, M.C., 2003. Regulation of pyruvate dehydrogenase complex activity by reversible phosphorylation. Biochem. Soc. Trans. 31, 1143–1151.

Jeong, J.Y., Jeoung, N.H., Park, K.G., Lee, I.K., 2012. Transcriptional regulation of pyruvate dehydrogenase kinase. Diabetes Metab. J. 36, 328–335.

Jose, C., Melser, S., Benard, G., Rossignol, R., 2013. Mitoplasticity: adaptation biology of the mitochondrion to the cellular redox state in physiology and carcinogenesis. Antioxid. Redox Signal. 18, 808–849.

Kimura, M., Takatsuki, A., Yamaguchi, I., 1994. Blasticidin S deaminase gene from Aspergillus terreus (BSD): a new drug resistance gene for transfection of mammalian cells. Biochim. Biophys. Acta 1219, 653–659.

Lin, S.C., Hardie, D.G., 2018. AMPK: sensing glucose as well as cellular energy status. Cell Metab. 27, 299–313.

Lindquist, C., Bjorndal, B., Rossmann, C.R., Tusubira, D., Svardal, A., Rosland, G.V., Tronstad, K.J., Hallstrom, S., Berge, R.K., 2017. Increased hepatic mitochondrial FA oxidation reduces plasma and liver TG levels and is associated with regulation of UCPs and APOC-III in rats. J. Lipid Res. 58, 1362–1373.

Liu, Z., Chen, X., Wang, Y., Peng, H., Wang, Y., Jing, Y., Zhang, H., 2014. PDK4 protein promotes tumorigenesis through activation of cAMP-response element-binding protein (CREB)-Ras homolog enriched in brain (RHEB)-mTORC1 signaling cascade. J. Biol. Chem. 289, 29739–29749.

Livak, K.J., Schmittgen, T.D., 2001. Analysis of relative gene expression data using real-time quantitative PCR and the 2(−Delta Delta C(T)) method. Methods 25, 402–408.

Manio, M.C., Inoue, K., Fujitani, M., Matsumura, S., Fushiki, T., 2016. Combined pharmacological activation of AMPK and PPARdelta potentiates the effects of exercise in trained mice. Physiol. Rep. 4.

Merrill, G.F., Kurth, E.J., Hardie, D.G., Winder, W.W., 1997. AICA riboside increases AMP-activated protein kinase, fatty acid oxidation, and glucose uptake in rat muscle. Am. J. Phys. 273, E1107–E1112.

Naviaux, R.K., Naviaux, J.C., Li, K., Bright, A.T., Alaynick, W.A., Wang, L., Baxter, A., Nathan, N., Anderson, W., Gordon, E., 2016. Metabolic features of chronic fatigue syndrome. Proc. Natl. Acad. Sci. U. S. A. 113, E5472–E5480.

Oie, E., Berge, R.K., Ueland, T., Dahl, C.P., Edvardsen, T., Beitnes, J.O., Bohov, P., Aukrust, P., Yndestad, A., 2013. Tetradecylthioacetic acid increases fat metabolism and improves cardiac function in experimental heart failure. Lipids 48, 139–154.

O'Neill, H.M., Lally, J.S., Galic, S., Thomas, M., Azizi, P.D., Fullerton, M.D., Smith, B.K., Pulinilkunnil, T., Chen, Z., Samaan, M.C., Jorgensen, S.B., Dyck, J.R., Holloway, G.P., Hawke, T.J., van Denderen, B.J., Kemp, B.E., Steinberg, G.R., 2014. AMPK phosphorylation of ACC2 is required for skeletal muscle fatty acid oxidation and insulin sensitivity in mice. Diabetologia 57, 1693–1702.

Pear, W.S., Nolan, G.P., Scott, M.L., Baltimore, D., 1993. Production of high-titer helper-free retroviruses by transient transfection. Proc. Natl. Acad. Sci. U. S. A. 90, 8392–8396.

Pin, F., Novinger, L.J., Huot, J.R., Harris, R.A., Couch, M.E., O'Connell, T.M., Bonetto, A., 2019. PDK4 drives metabolic alterations and muscle atrophy in cancer cachexia. FASEB J. 33, 7778–7790.

Roche, T.E., Hiromasa, Y., 2007. Pyruvate dehydrogenase kinase regulatory mechanisms and inhibition in treating diabetes, heart ischemia, and cancer. Cell. Mol. Life Sci. 64, 830–849.

Rohlenova, K., Veys, K., Miranda-Santos, I., De Bock, K., Carmeliet, P., 2018. Endothelial

cell metabolism in health and disease. Trends Cell Biol. 28, 224–236.
Rost, T.H., Haugan Moi, L.L., Berge, K., Staels, B., Mellgren, G., Berge, R.K., 2009. A pan-PPAR ligand induces hepatic fatty acid oxidation in PPARalpha−/− mice possibly through PGC-1 mediated PPARdelta coactivation. Biochim. Biophys. Acta 1791, 1076–1083.
Saxton, R.A., Sabatini, D.M., 2017. mTOR signaling in growth, metabolism, and disease. Cell 168, 960–976.
Sipula, I.J., Brown, N.F., Perdomo, G., 2006. Rapamycin-mediated inhibition of mammalian target of rapamycin in skeletal muscle cells reduces glucose utilization and increases fatty acid oxidation. Metabolism 55, 1637–1644.
Sugden, M.C., 2003. PDK4: a factor in fatness? Obes. Res. 11, 167–169.
Sugden, M.C., Holness, M.J., 1994. Interactive regulation of the pyruvate dehydrogenase complex and the carnitine palmitoyltransferase system. FASEB J. 8, 54–61.
Sugden, M.C., Bulmer, K., Gibbons, G.F., Holness, M.J., 2001. Role of peroxisome proliferator-activated receptor-alpha in the mechanism underlying changes in renal pyruvate dehydrogenase kinase isoform 4 protein expression in starvation and after refeeding. Arch. Biochem. Biophys. 395, 246–252.
Trexler, E.T., Smith-Ryan, A.E., Norton, L.E., 2014. Metabolic adaptation to weight loss: implications for the athlete. J. Int. Soc. Sports Nutr. 11, 7.
Tronstad, K.J., Nooteboom, M., Nilsson, L.I., Nikolaisen, J., Sokolewicz, M., Grefte, S., Pettersen, I.K., Dyrstad, S., Hoel, F., Willems, P.H., Koopman, W.J., 2014. Regulation and quantification of cellular mitochondrial morphology and content. Curr. Pharm. Des. 20, 5634–5652.
Turell, M.J., 1989. Effect of environmental temperature on the vector competence of Aedes fowleri for Rift Valley fever virus. Res. Virol. 140, 147–154.
Vigerust, N.F., Cacabelos, D., Burri, L., Berge, K., Wergedahl, H., Christensen, B., Portero-Otin, M., Viste, A., Pamplona, R., Berge, R.K., Bjorndal, B., 2012. Fish oil and 3-thia fatty acid have additive effects on lipid metabolism but antagonistic effects on oxidative damage when fed to rats for 50 weeks. J. Nutr. Biochem. 23, 1384–1393.
Wan, Z., Thrush, A.B., Legare, M., Frier, B.C., Sutherland, L.N., Williams, D.B., Wright, D.C., 2010. Epinephrine-mediated regulation of PDK4 mRNA in rat adipose tissue. Am. J. Physiol. Cell Physiol. 299, C1162–C1170.
Wensaas, A.J., Rustan, A.C., Lovstedt, K., Kull, B., Wikstrom, S., Drevon, C.A., Hallen, S., 2007. Cell-based multiwell assays for the detection of substrate accumulation and oxidation. J. Lipid Res. 48, 961–967.
Wensaas, A.J., Rustan, A.C., Just, M., Berge, R.K., Drevon, C.A., Gaster, M., 2009. Fatty acid incubation of myotubes from humans with type 2 diabetes leads to enhanced release of beta-oxidation products because of impaired fatty acid oxidation: effects of tetradecylthioacetic acid and eicosapentaenoic acid. Diabetes 58, 527–535.
Winder, W.W., Wilson, H.A., Hardie, D.G., Rasmussen, B.B., Hutber, C.A., Call, G.B., Clayton, R.D., Conley, L.M., Yoon, S., Zhou, B., 1997. Phosphorylation of rat muscle acetyl-CoA carboxylase by AMP-activated protein kinase and protein kinase a. J. Appl. Physiol. (1985) 82, 219–225.
Wu, P., Inskeep, K., Bowker-Kinley, M.M., Popov, K.M., Harris, R.A., 1999. Mechanism responsible for inactivation of skeletal muscle pyruvate dehydrogenase complex in starvation and diabetes. Diabetes 48, 1593–1599.
Wu, P., Blair, P.V., Sato, J., Jaskiewicz, J., Popov, K.M., Harris, R.A., 2000. Starvation increases the amount of pyruvate dehydrogenase kinase in several mammalian tissues. Arch. Biochem. Biophys. 381, 1–7.
Yamaguchi, S., Moseley, A.C., Almeda-Valdes, P., Stromsdorfer, K.L., Franczyk, M.P., Okunade, A.L., Patterson, B.W., Klein, S., Yoshino, J., 2018. Diurnal variation in PDK4 expression is associated with plasma free fatty acid availability in people. J. Clin. Endocrinol. Metab. 103, 1068–1076.